ՀԱՅԱՍՏԱՆԻ ԳԻՏՈՒԹՅՈՒՆՆԵՐԻ ԱԶԳԱՅԻՆ ԱԿԱԴԵՄԻԱՅԻ ՏԵՂԵԿԱԳԻՐ
ИЗВЕСТИЯ НАЦИОНАЛЬНОЙ АКАДЕМИИ НАУК АРМЕНИИ

Մեխանիկա 76, №3, 2023 Механика

УДК 539.3 **DOI: 10.54503/0002-3051-2023.76.3-6**

BAND GAP FORMATION IN A BEAM WITH ATTACHED LOCAL RESONATORS AND PERIODICALLY ARRANGED INTERMEDIATE EXTERNAL SUPPORTS

Ghazaryan K., Piliposyan G.

Keywords: Band gaps, localization, resonance frequency.

In the paper a comparative study of a band gap formation mechanism is presented in finite and infinite homogeneous beams rested on periodically arranged intermediate external supports and periodically attached local mass-spring resonators. The transfer matrix method in conjunction with Bloch-Floquet's approach is extended to study the flexural wave vibration and phonon band gaps generated by both of external intermediate supports and local resonators. The eigenvalue vibration problems are formulated for pinned and clamped multi-span finite length beams and the equation defining eigen frequencies are obtained. The novelty of the paper is the analytical and numerical results concerning formation of band gaps caused by local resonators and intermediate external supports.

Ղազարյան Կ., Փիլիփոսյան Գ.

Պարբերաբար տեղակայված արտաքին հենարաններին հենված և տեղային ռեզոնատորներով միացված հեծանի հաճախությունների արգելված գոտիների կազմավորվելը

Բանալի բառեր. արգելված գոտիներ, տեղայնացում, ռեզոնանսային հաճախություն:

Աշխատանքում ներկայացված է պարբերաբար տեղակայված միջանկյալ արտաքին հենարաններին հենված և տեղային ռեզոնատորներով միացված հեծանում հաճախությունների արգելված գոտիների կազմավորման համեմատական վերլուծությունը: Տրանսֆեր մատրիցների մեթոդի հետ զուգակցված, Բլոխ-Ֆլոկեի տեսության շրջանակում հետազոտված է արգելված գոտիների գոյացման մեխանիզմները՝ պայմանավորված ինչպես հենարաններով, այնպես էլ ռեզոնատորներով: Ձևակերպվել են եզրային խնդիրները և ստացվել են ամրակցված և հոդակապորեն հենված վերջավոր երկարության բազմաթռիչք հեծանների սեփական արժեքները որոշող հավասարումները:

Казарян К., Пилипосян Г.

Формирование запретных зон частот балки с присоединенными локальными резонаторами и опертой на периодически расположенные внешные опоры

Ключевые слова: запретные зоны, локализация, резонансная частота.

В работе представлен сравнительный анализ механизма образования запретных зон частот в балке с присоединенными локальными резонаторами и опертой на периодически расположенные промежуточные внешние опоры. В рамках теории Блоха-Флоке в сочетании метода трансфер матриц исследован механизм образования запретных зон, генерируемых как опорами так и резонаторами. Сформулированы краевые задачи и получены уравнения определяющие собственные частоты защемленных и шарнирно опертых многопролетных балок конечной длины.

1. Introduction

Periodic materials and structures, called mechanical metamaterials, demonstrate new physical properties unfeasible in naturally occurring materials [1,2]. Under certain conditions their frequency spectra exhibits band gaps, which are frequency ranges where wave propagation experiences significant attenuation [3–5]. This paper focuses on a particular class of a periodic structure, a periodic flexural beam, where periodicity can be achieved by a repeated variation along the axis of the beam, for example, by the presence of local resonators, which are normally either attached to the surface of the metamaterial structure or embedded inside [6–9].

Frequency bandgaps in metamaterial structures can be caused by local resonators or Bragg's scattering. In the first case local resonators absorb the kinetic energy from the oscillations propagating through the metamaterial structure [10]. When the frequency of the external vibration matches the resonant frequency of the local resonators the energy from these vibrations transfers to the local resonators [7]. On the other hand, Bragg's scattering bandgap forms due to the destructive interference and standing wave formation when the wavelength is multiple of the periodicity of the structure [11]. Bandgaps created by the presence of local resonators appear at much lower frequencies than the Bragg's frequencies [12, 13]. Frequency bandgaps in both cases have a wide range of application in vibration insulators, frequency filters, waveguides and energy harvesting [10, 14, and 15].

Wave propagating in beams may cause structural damages and inaccuracies in experimental measurements. Band gaps in beams can be used in engineering constructions for control of the behavior of waves since many engineering constructions are designed as one-dimensional periodically supported structures such as railway tracks, pipelines and multi-span bridges [16, 17]. Investigation the dynamic behavior of these structures are of great importance in minimizing their vibration response and failure, fatigue and damage and reducing the transmitted noise to the surrounding environment. Stronger vibration attenuation may also have applications in ambient vibration energy harvesting [18–20].

For infinite metamaterials the Bloch-Floquet theory is normally used to reduce the analysis of the wave propagation to the problem for a single unit cell [21]. Understanding the wave propagation in finitely periodic media is however more important for analyzing their acoustic properties, since most structures have a finite number of periodic cells. For finite periodic structures the problem becomes complicated and the transfer matrix approach with finite element method is often more suitable [22].

A typical example of a periodic structure is a uniform beam rested on external supports and local resonators [23]. In this paper the oscillatory response of wave propagation in such structure is investigated. Using the transfer matrix approach the problem is solved analytically by means of the Silvester's theorem.

2. Statement of the problem

Consider a dynamic problem of interaction of metabeams with both finite and infinite length with attached local resonators. The meta beam is rested on periodically arranged intermediate supports at points $x = (n-1)d$ and $x = nd$, (n = 1, 2, ...) and the local spring-mass resonators attached periodically at points $x = \left(n - 1/2\right)d$ (Fig.1).

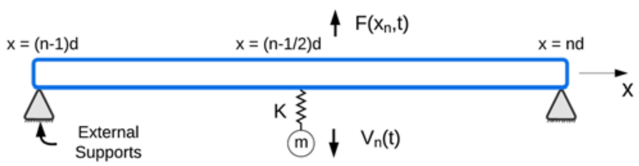

Fig. 1: The unit cell of the metabeam with external supports and local spring-mass resonators

The equation of motion of Euler-Bernoulli beam can be described by the following equation

$$EI\frac{\partial^4 W}{\partial x^4}+\rho A\frac{\partial^2 W}{\partial t^2}=0\,, \tag{1}$$

where $W(x,t)$ is the dynamic deflection of the beam, E is the elastic modulus, I is the area moment of inertia, ρ is the bulk density and A is the cross-section area.

The transverse interaction force $F(x_n,t)$ (Fig.1) of the beam with a local resonator of mass m attached at the points $x=x_n$ is given by the following formula [1]

$$F(x_n,t)=-m\frac{d^2V_n}{dt^2}\,, \tag{2}$$

where $V_n(t)$ is the vertical displacement of the resonator.

On the other hand we also have

$$K(W(x_n,t)-V_n(t))+m\frac{d^2V}{dt^2}=0, \tag{3}$$

where $W(x_n,t)$ is the displacement of the beam at point x_n, K (force per unit of length) is the resonator's spring stiffness.

Assuming functions in the form

$$W(x_n,t)=U(x_n)e^{i\omega t}\,,V_n=V_{0n}e^{i\omega t} \tag{4}$$

where ω is the frequency and substituting into (3) leads to

$$V_{0n}=\frac{K}{K-m\omega^2}U(x_n)\,. \tag{5}$$

Substituting (4) and (5) into (3) results in

$$F(x_n)=\frac{Km\omega^2}{K-m\omega^2}U(x_n) \tag{6}$$

In the basic unit cell $x\in((n-1)d,nd)$ the solutions for amplitude functions can be written as

$$U_{\pm}(x)\ =A_{1\pm}sin(px)\ +A_{2\pm}sinh(px)\ +A_{3\pm}cos(px)\ +A_{4\pm}cosh(px), \tag{7}$$

where $p=\sqrt{\rho A\omega(EI)^{-1}}$, subscripts $(\pm)$ denote regions:

$$(-)\rightarrow x\in(d(n-1),dn-d/2),\qquad ((+)\rightarrow x\in(dn-d/2,dn))$$

At each intermediate support the beam deflection is zero, the slope and the moment just to the left and to the right of the support are the same. These conditions at the support points in the unit cell can be written as

$$U_+(nd)=0\,,\ \left[\frac{dU_+(nd)}{dx}\right]=0\,,\left[\frac{d^2U_+(nd)}{dx^2}\right]=0 \tag{8}$$

$$U_-((n-1)d)=0\,,\ \frac{dU_-((n-1)d)}{dx}=0\,,\ \frac{d^2U_-((n-1)d)}{dx^2}=0 \tag{9}$$

where $[\cdot]$ is a jump of a function across the interfaces.

The interface conditions at the points $x_n = nd - d/2$ where the local resonators are attached can be cast as

$$U_+(x_n) = U_-(x_n)\ ,\ \frac{dU_+(x_n)}{dx} = \frac{dU_-(x_n)}{dx}$$
$$\frac{d^2U_+(x_n)}{dx^2} = \frac{d^2U_-(x_n)}{dx^2}\ ,\ \frac{d^3U_+(x_n)}{dx^3} - \frac{d^3U_-(x_n)}{dx^3} = fU_+(x_n) \quad (10)$$

where $f = \dfrac{Km\omega^2}{\left(K - m\omega^2\right)EI}$.

Introducing non-dimensional parameters: bending frequency of the beam $\Omega = \omega d^2\sqrt{\rho A(EI)}$, resonance frequency of the resonator $\Omega_0 = d^2\sqrt{(E\,\mathrm{Im})^{-1}A\tilde{n}K}$ and mass of the resonator $\mu = m(\rho Ad)^{-1}$, we rewrite parameter f as

$$f = \frac{\mu\Omega^2\Omega_0^2}{d^3\left(\Omega_0^2 - \Omega^2\right)} \quad (11)$$

The last condition of (10) provides a relationship between a local resonator and multi span beam rested on external supports.

3. Solution of the problem. Propagator matrix approach

In the unit cell the solutions (7) satisfying to the conditions (8) can be cast as

$$U_+(x) = A_{1+}\sin(pd(x-n)) + A_{2+}\sinh(pd(x-n)) +$$
$$+ A_{0+}(\cos(pd(x-n)) - \cosh(pd(x-n))),$$
$$U_-(x) = A_{1-}\sin(pd(x-n+1)) + A_{2-}\sinh(pd(x-n+1)) +$$
$$+ A_{0-}(\cos(pd(x-n+1)) - \cosh(pd(x-n+1))). \quad (12)$$

Substituting (12) into the interface conditions (11), the constants $A_{1\pm}$ and $A_{2\pm}$ can be expressed via $A_{0\pm}$ in the following way

$$A_{1-} = -\alpha(\gamma A_{0+} + \beta A_{0-}),\ A_{2-} = -\alpha(\vartheta A_{0+} + \theta A_{0-})$$
$$A_{1+} = \alpha(\beta A_{0+} + \gamma A_{0-}),\ A_{2+} = \alpha(\theta A_{0+} + \vartheta A_{0-}), \quad (13)$$

where

$$\alpha = (2f(\cot(\xi) - \coth(\xi)) + 8p^2\cot(\xi)\coth(\xi))^{-1}$$
$$\beta = \csc(\xi)\left(\csc(\xi)\coth(\xi)(4p^3\cos(2\xi) - f\sin(2\xi)) + f(\mathrm{csch}(\xi) + \cos(2\xi)\csc(\xi))\right)$$
$$\gamma = -\csc(\xi)\left(f\csc(\xi) - f\,\mathrm{csch}(\xi) + 4p^3\csc(\xi)\coth(\xi)\right),$$
$$\theta = \mathrm{csch}(\xi)\left(\cosh(2\xi)\mathrm{csch}(\xi)(f - 4p^3\cot(\xi))f\csc(\xi) - 2f\cot(\xi)\cosh(\xi)\right),$$
$$\vartheta = f\,\mathrm{csch}(\xi)(\csc(\xi) - \mathrm{csch}(\xi)) + 4p^3\cot(\xi)\mathrm{csch}^2(\xi),\quad \xi = \frac{pd}{2}.$$

Since the interface conditions at external supports are imposed on the functions $\frac{dU_{\pm}(x)}{dx}$ and $\frac{d^2U_{\pm}(x)}{dx^2}$ it is convenient to introduce the following column vectors

$$\mathbf{U}_{+}(x)=\left(\frac{dU_{\pm}(x)}{dx},\frac{d^2U_{\pm}(x)}{dx^2}\right)^T \tag{14}$$

Now expressing the vectors $\mathbf{U}_{+}(nd)$ and $\mathbf{U}_{+}((n-1)d)$ via the vector $\mathbf{A}=(A_{0-},A_{0+})^T$ we get

$\mathbf{U}_{+}(nd)=\mathbf{Q}_{+}\mathbf{A}$, $\mathbf{U}_{+}((n-1)d)\ =\mathbf{Q}_{-}\mathbf{A}$

where

$$\mathbf{Q}_{-}=\begin{pmatrix}-\frac{p(\beta+\theta)}{\alpha} & -\frac{p(\gamma+\vartheta)}{\alpha}\\ -2p^2 & 0\end{pmatrix},\ \mathbf{Q}_{+}=\begin{pmatrix}\frac{p(\beta+\vartheta)}{\alpha} & \frac{p(\gamma+\theta)}{\alpha}\\ 0 & -2p^2\end{pmatrix}$$

Excluding vector $\mathbf{A}=\mathbf{Q}^{-1}\mathbf{U}_{-}((n-1)d)$ we obtain the following relation

$$\mathbf{U}_{+}(nd)=\mathbf{M}\mathbf{U}_{-}((n-1)d), \tag{15}$$

where $\mathbf{M}=\mathbf{Q}_{+}\mathbf{Q}_{-}^{-1}$ and

$$\mathbf{M}=\frac{1}{\gamma+\vartheta}\begin{pmatrix}\theta-\beta & \frac{(\beta-\gamma+\theta-\vartheta)(\beta+\gamma+\theta+\vartheta)}{2\alpha p}\\ 2\alpha p & \theta-\beta\end{pmatrix} \tag{16}$$

Herein the matrix **M** is a unimodal propagator matrix for the Euler metabeam wave field, linking the vectors $\mathbf{U}_{+}(nd)$ and $\mathbf{U}_{-}((n-1)d)$ at the ends of the beam unit cell where the external supports are located and the local resonators are attached at the middle of the unit cell. Elements of matrix **M** in the explicit form can be written as

$$\mathbf{M}=\begin{pmatrix}m_{11} & m_{12}\\ m_{21} & m_{22}\end{pmatrix}$$

and

$$m_{11}=\Delta^{-1}\begin{pmatrix}\cos(pd)\left(f-4p^3\sinh(pd)\right)+\cosh(pd)\left(4p^3\sin(pd)-f\right)-\\ -4f\sin\left(\frac{pd}{2}\right)\sinh\left(\frac{pd}{2}\right)+2f\sin(pd)\sinh(pd)\end{pmatrix}; \tag{17}$$

$$m_{12}=p^{-1}\Delta^{-1}\begin{pmatrix}f\left(4\cos\left(\frac{pd}{2}\right)\sinh\left(\frac{pd}{2}\right)-(\cos(pd)+1)\sinh(pd)+2\sin(pd)\cosh^2\left(\frac{pd}{2}\right)\right)\\ +4p^3-4p^3\cos(pd)\cosh(p)+4f\sin\left(\frac{pd}{2}\right)\cosh\left(\frac{pd}{2}\right)\end{pmatrix}$$

(18)

$$m_{21}=\Delta^{-1}p\left(2\sinh(pd)\left(f(\cos(pd)-1)+4p^3\sin(pd)\right)+4f\sin(pd)\sinh^2\left(\frac{pd}{2}\right)\right);m_{22}=m_{11}$$

$$\Delta=f\left(\cos(pd)-\cosh(pd)+4\sin\left(\frac{pd}{2}\right)\sinh\left(\frac{pd}{2}\right)\right)+4p^3\left(\sin(pd)-\sinh(pd)\right);$$

(19)

If the resonators are absent $f=0$ then

$$\mathbf{M}_0==\begin{pmatrix}\dfrac{\sin(pd)\cosh(pd)-\cos(pd)\sinh(pd)}{\sin(pd)-\sinh(pd)} & \dfrac{1-\cos(pd)\cosh(pd)}{p\sin(pd)-p\sinh(pd)}\\ \dfrac{2p\sin(pd)\sinh(pd)}{\sin(pd)-\sinh(pd)} & \dfrac{\sin(pd)\cosh(pd)-\cos(pd)\sinh(pd)}{\sin(pd)-\sinh(pd)}\end{pmatrix}$$

(20)

The matrix $\mathbf{M}_0$ links the vectors $\mathbf{U}_+(nd)\ =\mathbf{M_0U}_+((n-1)d)$ at the ends of the *n*-th cell where the external support are placed only.

4. Finite and infinite length meta beams, Sylvester's theorem

The elements of this matrix $\mathbf{M}$ are independent of the unit cell number, and since the vectors $\mathbf{U}_+(nd)$ and $\mathbf{U}_-((n-1)d)$ are continuous at the supports points of the neighboring cells, repeating relations (15) *n* times the propagator unimodal matrix $\mathbf{M}^n$ can be found. For any *n = 1, 2, .., N* the matrix $\mathbf{M}^n$ links the beam deflections and slopes at *x = 0* and *x = nd.*

$$\mathbf{U}_+\left(nd\right)=\mathbf{M}^nU_-\left(0\right). \tag{21}$$

According to Sylvester's matrix polynomial theorem [24] the elements of the *n*-th power of a 2 × 2 unimodal matrix $M=\{m_{ij}\}^2_{i,j=1}$ can be expressed as

$$\mathbf{M}^n=\begin{pmatrix}M_{11}(n) & M_{12}(n)\\ M_{21}(n) & M_{22}(n)\end{pmatrix} \tag{22}$$

where

$$M_{11}(n)=m_{11}S_{n-1}(\eta)-S_{n-2}(\eta),\quad M_{12}(n)=m_{12}S_{n-1}(\eta),$$
$$M_{21}(n)=m_{21}S_{n-1}(\eta),\quad M_{22}(n)=m_{22}S_{n-1}(\eta)-S_{n-2}(\eta) \tag{23}$$

and $S_n(\eta)$ are the Chebyshev polynomials of second kind, namely

$$S_n(\eta)=\frac{\sin((n+1)\arccos(\eta))}{\sin(\arccos(\eta))},\ \eta=\frac{m_{11}+m_{22}}{2} \tag{24}$$

The relation establishing a link between values of the vectors $\mathbf{U}_+(L)$ and $\mathbf{U}_-\left(0\right)$ will enable to solve the boundary problems of free and forced vibration of metabeam. The following three boundary problems can be solved for beam with periodically arranged supports: clamped–clamped, hinged-hinged, hinged-clamped at x = 0 and x = L.

In the case of the clamped-clamped metabeam the following matrix equation can be imposed

$$\begin{pmatrix} 0 \\ \dfrac{d^2U_+(L)}{dx^2} \end{pmatrix} = \begin{pmatrix} M_{11} & M_{12} \\ M_{21} & M_{22} \end{pmatrix} \begin{pmatrix} 0 \\ \dfrac{d^2U_+(0)}{dx^2} \end{pmatrix} \tag{25}$$

From the non-trivial solutions of (25) one can find the following frequency equation

$$M_{12}(\omega,\eta) = 0 \tag{26}$$

For a simply hinged-clamped metabeam based on matrix equation

$$\begin{pmatrix} \dfrac{d^2U_+(L)}{dx^2} \\ 0 \end{pmatrix} = \begin{pmatrix} M_{11} & M_{12} \\ M_{21} & M_{22} \end{pmatrix} \begin{pmatrix} 0 \\ \dfrac{d^2U_+(0)}{dx^2} \end{pmatrix} \tag{27}$$

the following frequency equation can be cast as

$$M_{22}(\omega,\eta) = 0 \tag{28}$$

For a hinged-hinged metabeam from matrix equation

$$\begin{pmatrix} \dfrac{d^2U_+(L)}{dx^2} \\ 0 \end{pmatrix} = \begin{pmatrix} M_{11} & M_{12} \\ M_{21} & M_{22} \end{pmatrix} \begin{pmatrix} \dfrac{d^2U_+(0)}{dx^2} \\ 0 \end{pmatrix} \tag{29}$$

the following frequency equation can be cast as

$$M_{12}(\omega,\eta) = 0 \quad (30)$$

The equations (26), (28) and (30) define the eigenfrequencies of a beam of finite length *L=Nd* rested on *N +1* external supports with attached *N* local mass-spring resonators. Investigation of these equations is the aim of our future studies and will not consider here.

Applying the Bloch-Floquet quasi periodicity condition at both ends of the unit cell

$$\mathbf{U}_+(nd) = \lambda \mathbf{U}_-((n-1)d) \tag{31}$$

where $\lambda = exp(ikd)$, k is the Bloch–Floquet wave number, and taking into account (15) we come to following matrix eigenvalue problem

$$(\mathbf{M} - \lambda \mathbf{I})\mathbf{U}_-((n-1)d) = 0 \tag{32}$$

It follows from (32) that the eigenvalues of the periodic structure satisfy the following equation:

$$\lambda^2 - 2\lambda\eta + 1 = 0 \,,\ \eta = m_{11} \tag{33}$$

Taking into account (33) the equation defining the gaps of the infinite beam with external supports and local resonators can be written as

$$\cos(kd) = m_{11} = \eta(\mu,\Omega,\Omega_0) \tag{34}$$

where

$$\eta(\mu,\Omega,\Omega_0) = \Phi K^{-1}$$

$$\Phi = \Omega_0^2(\mu r(\cos(r) - \cosh(r) - 4\sin(r/2)\sinh(r/2) + 2\sin(r)\sinh(r))$$
$$-4\cos(r)\sinh(r) + 4\sin(r)\cosh(r)) + 4\Omega^2(\cos(r)\sinh(r) - \sin(r)\cosh(r));$$
$$K = \Omega_0^2(4(\sin(r) - \sinh(r)) - 2\mu r(\sin(r/2) - \sinh(r/2))^2) - 4\Omega^2(\sin(r) - \sinh(r))$$
$$, r = \sqrt{\Omega}$$

The deviation the function $\eta(\mu, \Omega, \Omega_0)$ defines gaps in both infinite beam and eigen frequencies of a finite beam given by equations (26), (28) and (30).

5. Analysis, discussion and numerical results

The condition $|\eta(\mu, \Omega, \Omega_0)| > 1$ defines band gaps in an infinite beam. When resonators are absent ($\mu = 0$), it follows from (17) that

$$\eta_0 = \frac{\sin\left(\sqrt{\Omega}\right)\cosh\left(\sqrt{\Omega}\right) - \cos\left(\sqrt{\Omega}\right)\sinh\left(\sqrt{\Omega}\right)}{\sin\left(\sqrt{\Omega}\right) - \sinh\left(\sqrt{\Omega}\right)} \tag{35}$$

Dispersion curves defining band gaps in the first Brillouin zone for a beam without resonators rested on periodically arranged supports, are presented in Figure 2. Figure 2a shows the band structure of frequency Ω versus the real part of a Bloch wave vector *kd*, the dashed horizontal lines on dispersion curves determine the bounds of the first four gaps $\Omega \in (22.3, 39.4)$, $\Omega \in (61.6, 88.7)$, $\Omega \in (120.7, 157.7)$ and $\Omega \in (200.8, 248.7)$. There is also a cut-off frequency at $\Omega = 9.6$ below which the waves cannot propagate.

Figure 2b presents the complex band of the real and imaginary parts of the Bloch wave vector *kd* versus frequency Ω. Solid blue curves correspond to the real part of the

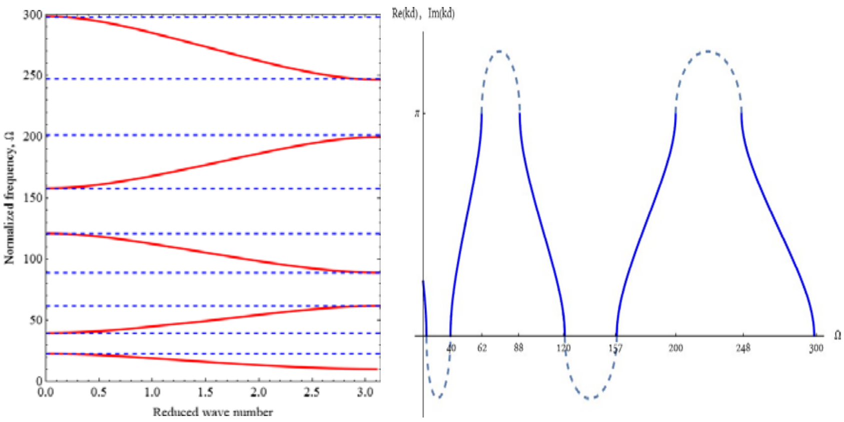

(a) Band structure of Ω versus the real part of *kd,* (b) Complex hybrid band structure of real (solid blue) and *kd* imaginary (dashed) parts of *kd* versus frequency

Bloch wave vector kd in the first Brillouin zone kd ∈ (0, π), dashed symmetric curves correspond to the imaginary part of the Bloch wave vector.

The imaginary parts of the Bloch vector Im(kd) define the attenuation of the flexible waves whose frequencies are inside the bandgaps, while the real part of the Bloch vector Re(kd) defines the dispersion of the flexible waves whose frequencies are outside the bandgaps [25].

Figure 3. shows the plots of the beam resonance frequency Ω_r for $\eta(\mu, \Omega_r, \Omega_0) \to \infty$ as a function of the local resonator frequency Ω_0 for different values of μ, where δ is the resonance width for given values of Ω_0 and μ. As it follows from Fig. 3 the beam resonance frequencies depend on the resonator mass and do not coincide with local resonator frequencies $\Omega_r \neq \Omega_0$. The resonator mass increases the beam resonance frequency. In the case of μ = 0.1 the beam resonance frequency Ω_r practically coincides with local resonator frequency Ω_0.

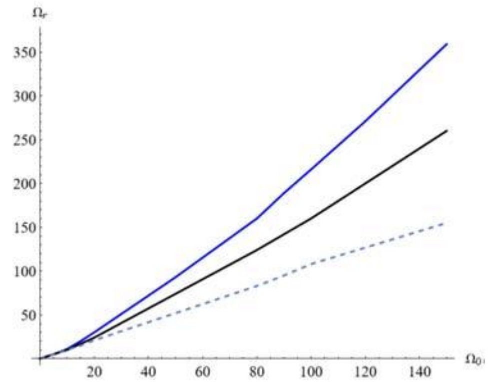

Fig. 3: The beam resonance frequency Ω_r as function of local resonator frequency Ω_0.
The blue, black and dashed curves correspond to μ = 1, μ = 0.5, and μ = 0.2 correspondingly.

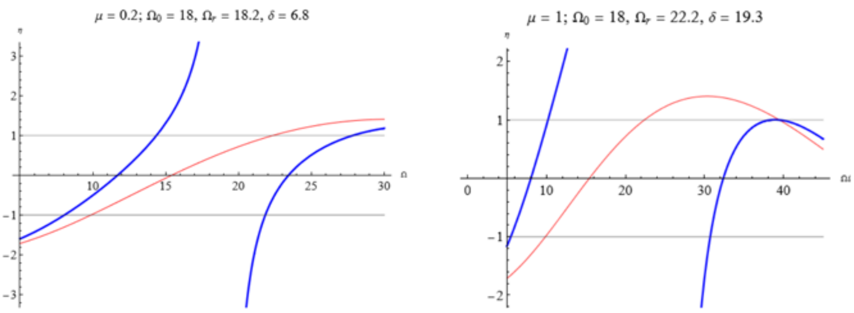

Fig. 4: The plots of the derivation function $\eta(\mu,\Omega,\Omega_0)$ at the beam resonance frequencies Ω_r

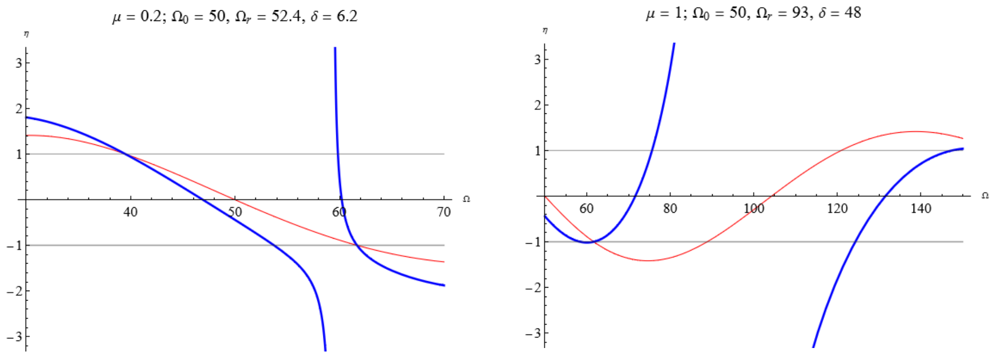

Fig. 5: The plots of the derivation function $\eta(\mu,\Omega,\Omega_0)$ at the beam resonance frequencies Ω_r.

On the Figures 4 and 5 the plots of the deviation functions $\eta(\mu,\Omega,\Omega_0)$ are presented in the neighborhood of the resonance frequencies Ω_r which are not coinciding with the resonator resonance frequencies Ω_r, $\Omega_r \neq \Omega_0$, δ is the resonance width for given values of Ω_0. Blue and red curves correspond to a beam with and without resonator:

1) Fig. 4 (a,b) at the resonator resonance frequency $\Omega_0 = 18$ in the case of two different masses of the resonator $\mu = 1$ and $\mu = 0.2$,

2) Fig 5 (a,b) at resonance frequency $\Omega_0 = 50$ in the case of two different masses of the resonator $\mu = 1$ and $\mu = 0.2$.

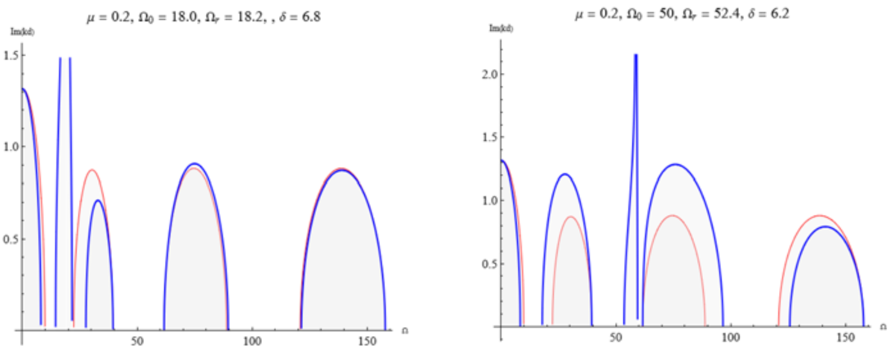

Fig. 6: Attenuation curves versus frequency in the range $\Omega \in (0, 250)$ illustrating the variation of band gap width caused by the local resonators.

As it follows from Figures 4 and 5 at resonance frequencies new bandgaps open with widths δ significantly depending on the mass of the resonator and the resonance frequency.

Since the imaginary parts of the Bloch vector Im(kd) operate inside the bandgaps, the analysis of the bandgap structure caused by a local resonator will be carried out by considering the attenuation function (Im(kd) in the bandgaps. The influence of the resonator resonance frequency Ω_0 on the formation of band gaps is illustrated in Figures 6 and 7 where the imaginary parts (attenuation curves) of the Bloch wave vectors are plotted as a function of Ω in the range Ω ∈ (0.250). Blue curves correspond to the multi span beam with resonators and red curves to the beam without resonators. In Figures 6 and 7 the lowest contours of the attenuation curves where Im(kd) → 0 define the map of bandgap frequencies.

It follows from Figures 6 and 7, that for a local resonator of a small mass $\mu = 0.2$ at resonance frequencies new bandgaps open only in their neighborhood. But for the resonator with a mass $\mu = 1$ new broader band gaps also open both above and below of resonance frequencies. Note that dimensionless mass μ is the ratio of the local resonator's mass and the mass of the beam unit cell. As it follows from Figures 6 and 7 the attenuation curves within a resonance bandgaps are not symmetrical while the attenuation curves describing bandgaps due to supports are symmetrical.

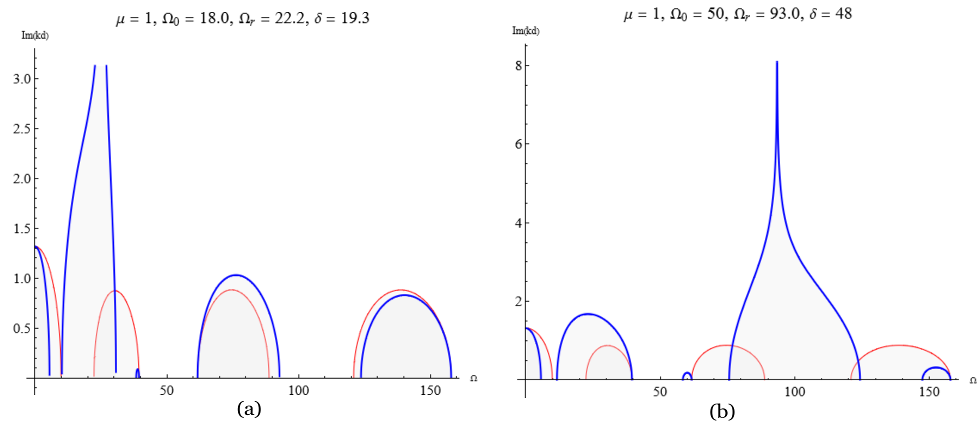

Fig. 7 Attenuation curves versus frequency in the range $\Omega \in (0,150)$ illustrating the variation of band gap width caused by the local resonators.

6. Conclusion

A locally resonant homogeneous multi span beam rested on periodically arranged intermediate supports with periodically attached spring–mass resonators is studied in this work. The transfer matrix method in conjunction with Bloch-Floquet's approach is extended to study the flexural wave vibration and bandwidth of a metabeam phononic band gaps generated by both of external intermediate supports and local resonators. The eigenvalue problems for the free vibration study is formulated for finite length pinned and clamped multi-span beams. For an infinite beam explicit analytical formulations are provided defining the bandgap formation. It is demonstrated that two types of band gaps, due to resonance and external supports, co-exist in the beam. It is shown that the beam resonance frequencies depend on the mass of resonators and do not coincide with local resonator frequencies. The resonator mass increases the beam resonance frequency. The local resonator of small mass opens new band gaps only in the neighborhood of the resonance frequencies. If the mass of the resonator is comparable with the mass of the beam's unit cell new and wider bandgaps open up both above and below of resonance frequencies.

Acknowledgments
The work was supported by the State Committee of Science of RA, in the framework of the research project 21T-2C299.

References

1. Yu, D., Liu, Y., Wang, G., Zhao, H., Qiu, J. (2006). Flexural vibration band gaps in Timoshenko beams with locally resonant structures. Journal of applied physics, 100(12).
2. Matlack, K. H., Bauhofer, A., Krödel, S., Palermo, A., and Daraio, C. (2016). Composite 3D-Printed Metastructures for Low-Frequency and Broadband Vibration Absorption. Proc. Natl. Acad. Sci. USA Vol. 113(30), pp. 8386-8390.
3. Adams, S., Craster R.V., Guenneau S. (2008). Bloch waves in periodic multi-layered acoustic layers, Proceedings of the Royal Society of London A: Mathematical, Physical and Engineering Sciences. Vol. 464. No. 2098.
4. Hussein M.I., Leamy M.J., Ruzzene M. (2014). Dynamics of phononic materials and structures: historical origins, recent progress, and future outlook, Applied Mechanics Reviews, 66, 040802/1-38.
5. Casablanca, O., Ventura, G., Garesc`ı, F., Azzerboni, B., Chiaia, B., Chiappini, M., et al. (2018). Seismic Isolation of Buildings Using Composite Foundations Based on Metamaterials. J. Appl. Phys. 123 No. 17.
6. Patro, S. R., Banerjee, A., Ramana, G. V. (2023). Vibration attenuation characteristics of finite locally resonant meta beam: Theory and experiments. Engineering Structures, 278, 115506.
7. Anigbogu, W., Nguyen, H. and Bardaweel, H.(2021). Layered Metamaterial Beam Structures With Local Resonators for Vibration Attenuation: Model and Experiment. Frontiers in Mechanical Engineering, Vol. 7, p.768508.
8. Liu, Z., Zhang, X., Mao, Y., Zhu, Y. Y., Yang, Z., Chan, C. T., et al. (2000). Locally Resonant Sonic Materials. Science, 289. 1734–1736.
9. Failla,G., Santoro R., Burlon A., Russillo A. (2020). An exact approach to the dynamics of locally-resonant beams, Mechanics Research Communications, Vol. 103, 103460.
10. Li, Y., Baker, E., Reissman, T., Sun, C., and Liu, W. K. (2017). Design of Mechanical Metamaterials for Simultaneous Vibration Isolation and Energy Harvesting. Appl. Phys. Lett. 111 (25), 251903.
11. Kushwaha, M. S., Halevi, P., Dobrzynski, L., and Djafari-Rouhani, B. (1993). Acoustic Band Structure of Periodic Elastic Composites. Phys. Rev. Lett. 71 (13), 2022–2025.
12. Liu, Z., Chan, C. T., and Sheng, P. (2005). Analytic Model of Phononic Crystals with Local Resonances. Phys. Rev. B 71 No.1, 14103.
13. Botshekan M., Tootkaboni M., Louhghalam A. (2019). On the dynamics of periodically restrained flexural structures under moving loads, International Journal of Solids and Structures, Vol. 180–181, pp. 62-71,
14. Piliposian G., Hasanyan A., Piliposyan G., Jilavyan H. (2020). On the Sensing, Actuating and Energy Harvesting Properties of a Composite Plate with Piezoelectric Patches, International Journal of Precision Engineering and Manufacturing-Green Technology, Vol.7, pp. 657–668.

15. Reichl, K. K., and Inman, D. J. (2017). Lumped Mass Model of a 1D Metastructure for Vibration Suppression with no Additional Mass. J. Sound Vibration Vol. 403 pp. 75–89.
16. Gry L., Gontier C., Dynamic Modelling of Railway Track: A Periodic Model Based on a Generalized Beam Formulation, Journal of Sound and Vibration, Vol. 199(4), pp. 531-558,
17. Garc´ıa-Palacios J, Samart´ın A, Melis M. (2012), Analysis of the railway track as a spatially periodic structure. Proc. of the Institution of Mechanical Engineers, Part F: Journal of Rail and Rapid Transit. 226(2), pp.113-123.
18. Anigbogu, W., Bardaweel, H. (2020). A metamaterial inspired structure for simultaneous vibration attenuation and energy harvesting. Shock and Vibration, v.2020. Article ID 4063025, p.1-12
19. Motaei, F., Bahrami, A. (2022). Energy harvesting from sonic noises by phononic crystal fibers. Scientific Reports, 12(1), 1-8.
20. Ma, T. X., Fan, Q. S., Zhang, C., Wang, Y. S. (2022). Flexural wave energy harvesting by the topological interface state of a phononic crystal beam. Extreme Mechanics Letters, 50, 101578.
21. Chen J., Chao I., Chen T. (2022). Bandgaps for flexural waves in infinite beams and plates with a periodic array of resonators, Journal of Mechanics, Vol 38, pp. 376–389.
22. Kobayashi F., Biwa S., Ohno N. (2004). Wave transmission characteristics in periodic media of finite length: multilayers and fiber arrays. International journal of solids and structures, 41(26), pp.7361-7375.
23. Avetisyan A., Ghazaryan K., Marzocca P. (2023). Stability of a finite length multi-span beam resting on periodic rigid and elastic supports, International Journal of Solids and Structures, Vol. 281, 112410, ISSN 0020-7683.
24. Tovar A.A., Casperson, W., (1995), Generalized Sylvester theorems for periodic applications in matrix optics, J. Opt. Soc. Am. A 12, p.578-590.
25. Nougaoui, A., Rouhani, B. D. (1988). Complex band structure of acoustic waves in superlattices. Surface science, 199(3), 623-637.

Information about authors

Ghazaryan K., Institute of Mechanics NAS Armenia E-mail: ghkarren@gmail.com

Piliposyan G., Institute of Mechanics NAS Armenia. E-mail: piliposyan.gor@gmail.com

Received 22.07.2023